Tohoku J. Exp. Med., 2023, **261**, 211-219

Cell Division Control Protein 42 Facilitates Diabetic Retinopathy Progression by Activating the MEK/ERK Pathway

Hui Cao[1,*] and Changzheng Hou[2,*]

[1]Department of Ophthalmology, The Affiliated Changsha Central Hospital, Hengyang Medical School, University of South China, Changsha, Hunan, China
[2]Department of Anesthesiology, The Third Xiangya Hospital of Central South University, Changsha, Hunan, China

Cell division control protein 42 (CDC42) modulates insulin secretion and angiogenesis to participate in the pathology of diabetic complications and retinal vascular-associated diseases. This study intended to explore the role of CDC42 in the progression of diabetic retinopathy, and the underlying mechanism. Human retinal microvascular endothelial cells (hRMECs) were cultured in 5.5 mM glucose (normal glucose) or 25 mM glucose (high glucose; HG) medium, respectively. CDC42 overexpression plasmid and small interference RNA (oe-CDC42 and si-CDC42) or corresponding negative controls (oe-NC and si-NC) were transfected into hRMECs under HG. Then, platelet-activating factor C-16 (C16-PAF) (MEK/ERK pathway activator) was added to si-CDC42 or si-NC transfected hRMECs under HG. Our study showed that HG increased CDC42 mRNA and protein, cell viability, invasive cell count, branch points, and tube length but reduced cell apoptosis in hRMECs. CDC42 upregulation enhanced cell viability, invasive cell count, branch points, tube length, p-MEK, and p-ERK, but attenuated cell apoptosis. Downregulation of CDC42 exhibited opposite trends. In addition, C16-PAF also increased cell viability, invasive cell count, branch points, and tube length, p-MEK, and p-ERK, but retarded cell apoptosis. Notably, C16-PAF diminished the effect of CDC42 downregulation on the above-mentioned functions in hRMECs under HG. Conclusively, CDC42 promotes HG-induced hRMEC viability and invasion, as well as angiogenesis, but inhibits apoptosis by activating the MEK/ERK pathway, which may be responsible for the progression of diabetic retinopathy.

Keywords: angiogenesis; cell division control protein 42; cell viability and invasion; diabetic retinopathy; MEK/ERK pathway
Tohoku J. Exp. Med., 2023 November, **261** (3), 211-219.
doi: 10.1620/tjem.2023.J068

Introduction

Diabetic retinopathy (DR) is a common microvascular complication of diabetes, which may cause vision loss and greatly impacts patients' quality of life (Tan and Wong 2023). Globally, the prevalence of DR ranges from 13.37% to 35.90% in diabetes patients, and it is estimated that more than 100 million adults have DR in 2020 (Teo et al. 2021). Treatments for DR include laser therapy, vitrectomy, anti-vascular endothelial growth factor (VEGF) drugs, and steroids, which have made certain progress in improving the outcomes of DR patients (Stitt et al. 2016; Everett and Paulus 2021; Liu and Wu 2021). However, none of these treatments could completely mitigate the clinical progression of retinal damage, and many DR patients do not respond well to certain treatments, resulting in a poor visual outcome (Stitt et al. 2016; Whitehead et al. 2018; Khan et al. 2020; Schreur et al. 2021; Purola et al. 2022). Thus, exploring potential therapeutic targets that attenuate retinal damage is crucial to improve the clinical outcomes of DR patients.

Cell division control protein 42 (CDC42) is a member of the Rho GTPases family, which has been found to participate in the modulation of diabetic complications and retinal vascular diseases (Huang et al. 2019; Uemura and Fukushima 2021). According to a study, CDC42 is upregu-

Received July 3, 2023; revised and accepted August 6, 2023; J-STAGE Advance online publication August 25, 2023
*These two authors contributed equally to this work.
Correspondence: Hui Cao, Department of Ophthalmology, The Affiliated Changsha Central Hospital, Hengyang Medical School, University of South China, No.161 Shaoshan South Road, Yuhua District, Changsha, Hunan 410013, China.
e-mail: chuangpujiuoc@163.com

lated under high glucose (HG), which further causes podocyte apoptosis and attenuates β-cell insulin secretion in type 2 diabetic nephropathy mice (Jiang et al. 2022). In addition, another study reports that HG-induced CDC42 participates in the change of the number and length of filopodia in podocytes, which is responsible for the pathology of diabetic nephropathy (Shen et al. 2016). In terms of the role of CDC42 in retinal vascular development, CDC42 is responsible for endothelial tip cell selection, directed cell migration, and filopodia formation in postnatal mouse retinas (Lavina et al. 2018). At the same time, CDC42 activation promotes actin polymerization and cell motility thereby facilitating retinal angiogenesis in endothelial cells (Kusuhara et al. 2012). Notably, exposure to HG leads to retinal endothelial cell proliferation and invasion, which further accelerates DR progression. After that, retinal capillaries become nonperfused, leading to retinal ischemia. The ischemic retina further secretes VEGF, which promotes vascular permeability, ultimately leading to angiogenesis (Chaudhary et al. 2021). Considering that retinal cell proliferation, invasion, and angiogenesis play an important role in DR progression, it is speculated that CDC42 may also engage in DR progression (Antonetti et al. 2021). However, relevant evidence is scarce.

The present study aimed to explore the involvement of CDC42 in DR progression, and the underlying mechanism.

Methods

Cell culture

Human retinal microvascular endothelial cells (hRMECs; Cell Systems, Kirkland, WA, USA) were cultured in 10% fetal bovine serum (FBS; Sigma, St. Louis, MO, USA) containing Dulbecco's Modified Eagle Medium (DMEM; Sigma). A humidity condition of 5% CO_2 at 37°C was provided. The hRMECs cultured with 5.5 mM glucose (catalog number: D6046; Sigma) or 25 mM glucose medium (catalog number: D0822; Sigma) were catalogued as normal glucose (NG) or HG group (Ji et al. 2022).

Transfection and C16-PAF incubation

The hRMECs (5×10^5) in HG group were transfected with 0.8 ng overexpression plasmid and 50 pM small interference RNA (siRNA) of CDC42 (oe-CDC42 and si-CDC42; GenePharma, Shanghai, China) or corresponding negative controls (oe-NC and si-NC, GenePharma) in the presence of Hilymax (Dojindo, Kumamoto, Japan) at 37°C. The non-transfected hRMECs were set as control. At 48 hours (h), the subsequent detections including reverse transcription quantitative polymerase chain reaction (RT-qPCR), immunoblotting, cell counting kit-8 (CCK-8), TUNEL, Transwell and tube formation assays were conducted. After transfection of si-CDC42 or si-NC, the hRMECs was stimulated by platelet-activating factor C-16 (C16-PAF; Yeasen, Shanghai, China) with an amount of 10 nM (Xia et al. 2022; You et al. 2022). After 48 h, the detections mentioned above were carried out.

Real-time quantitative polymerase chain reaction (RT-qPCR)

To complete RNA isolation, the RNApure kit (CWBIO, Beijing, China) was applied. The cDNA Synthesis Kit (CWBIO) and UltraSYBR One Step RT-qPCR Kit (CWBIO) were adopted to complete reverse transcription and qPCR, respectively. The primers were presented as follow: CDC42 forward, 5′-GGCGATGG TGCTGTTGGTAA-3′; CDC42 reverse, 5′-GCGGTCGT AATCTGTCATAATCCT-3′; GAPDH forward, 5′-GAGT CCACTGGCGTCTTCAC-3′, GAPDH reverse, 5′-ATCTT GAGGCTGTTGTCATACTTCT-3′. With GAPDH being used as internal reference, the results were calculated by $2^{-\Delta\Delta Ct}$ method (Yuan et al. 2006).

Immunoblotting

Nuclear and Cytoplasmic Extraction Kit (CWBIO, Taizhou, China) and BCA Protein Assay Kit (CWBIO) were applied to lyse cells and quantify protein, accordingly. A 4-20% precast gel (Willget, Shanghai, China) was used to separate protein. The protein was subsequently transferred to nitrocellulose membrane. After being blocked by 5% bovine serum albumin (BSA; Servicebio, Wuhan, China), the membrane was incubated with primary antibodies overnight at 4°C, followed by incubating with goat anti-rabbit secondary antibody (1:5,000, Servicebio) for 1.5 h at 37°C. At last, the membrane was visualized by ECL kit (Servicebio). The primary antibody of CDC42 (Protech, Wuhan, China), MEK (1:5,000, Protech), p-MEK (1:2,000; Cell Signaling Technology, Danvers, MA, USA), ERK (1:5,000, Protech), p-ERK (1:2,000; Cell Signaling Technology) and GAPDH antibody (1:2,000, Servicebio).

CCK-8, TUNEL and Transwell

The cell viability was assessed by CCK-8. In brief, CCK-8 reagent (Servicebio) was incubated with cells for 2 h. The optical density at 450 nm was measured by a microplate reader (Biotek, Winooski, VT, USA). The cell apoptosis was analyzed by TUNEL kit (Beyotime, Nantong, China). In brief, the cells were incubated with TUNEL working solution for 1 h after being fixed in 4% paraformaldehyde. The pictures were taken after the nucleus being stained by 4',6-diamidino-2-phenylindole (DAPI). The proportion of apoptotic cells was assessed by the following formula: number of red spots/number of blue spots × 100%. The invasion ability was assessed by Transwell. In brief, the resuspended cells, which were in 1% FBS containing DMEM, were seeded in matrix matrigel (Yeasen) pe-coated transwell insert for 24 h. Afterwards, the invaded cells were stained by crystal violet (Servicebio) and counted under an inverted microscope (Motic, Xiamen, China) with 3 pictures were taken.

Tube formation assays

In brief, the 96-well plates were coated by matrix matrigel (Yeasen) overnight. Then, the resuspended single cells were planted on plates for 12 h. The images with an amount of 3 were captured by an inverted microscope (Motic).

Data analysis

Graphpad Prism 9.0 (GraphPad Software, Boston, MA, USA) was used to analysis data, which were expressed as mean ± standard deviation (SD). All experiments were triplicated. Unpaired t-test or one-way ANOVA followed by Tukey's multiple comparison was applied to determine the difference of groups. *P* value less than 0.05 was considered as statistically significance.

Results

Effect of HG in hRMECs

CDC42 mRNA was increased in the HG group vs. the NG group ($P < 0.01$) (Fig. 1A). CDC42 protein was detected by immunoblotting (Fig. 1B), which suggested that CDC42 protein was elevated in the HG group compared to the NG group ($P < 0.05$) (Fig. 1C). Cell viability was elevated in the HG group vs. the NG group ($P < 0.05$) (Fig. 1D). TUNEL, Transwell, and tube formation assays were performed and cell apoptosis, invasive cell count, branch points, and tube length were analyzed (Fig. 1E). In detail, cell apoptosis ($P < 0.05$) (Fig. 1F) was decreased, while invasive cell count ($P < 0.05$) (Fig. 1G), branch points ($P < 0.05$) (Fig. 1H), and tube length ($P < 0.01$) (Fig. 1I) were increased in the HG group vs. the NG group.

Effect of CDC42 on cell viability, apoptosis, invasion, and angiogenesis in hRMECs under HG

CDC42 mRNA level was increased in the oe-CDC42 group vs. the oe-NC group ($P < 0.001$) but decreased in the si-CDC42 group vs. the si-NC group ($P < 0.01$) (Fig. 2A). By immunoblotting (Fig. 2B), CDC42 protein level was also increased in the oe-CDC42 group vs. the oe-NC group ($P < 0.001$), while reduced in the si-CDC42 group compared to the si-NC group ($P < 0.01$) (Fig. 2C). These findings indicated the transfection was successful. Cell viability was enhanced in the oe-CDC42 group vs. the oe-NC group ($P < 0.05$) but decreased in the si-CDC42 group vs.

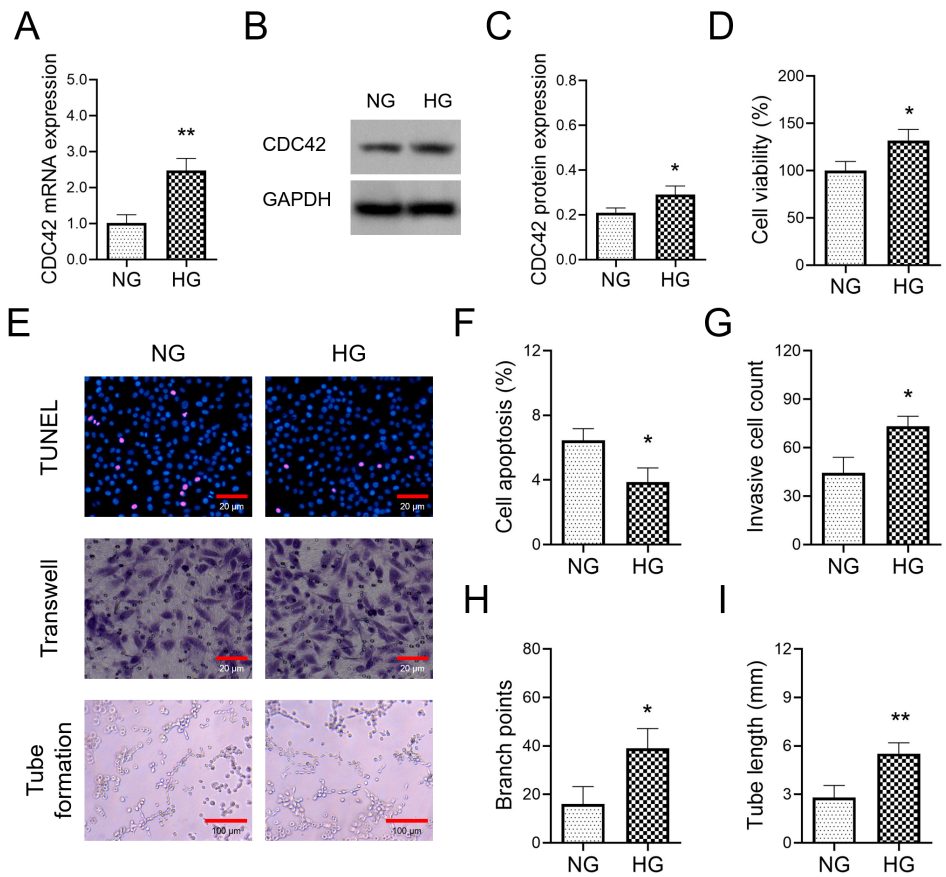

Fig. 1. High glucose (HG) facilitated CDC42 overexpression and diabetic retinopathy (DR) progression.
CDC42 mRNA (A), representative images of CDC42 protein by immunoblotting (B), CDC42 protein (C), cell viability (D), representative images of cell apoptosis, invasion, and branch points/tube length by TUNEL, Transwell, and tube formation assays, respectively (E), cell apoptosis (F), invasive cell count (G), branch points (H), and tube length (I) were compared between the normal glucose (NG) and HG groups. The experiments were triplicated. Statistical analysis was performed by Student's t-test. *P < 0.05, **P < 0.01

the si-NC group ($P < 0.01$) (Fig. 2D). Cell apoptosis was decreased in the oe-CDC42 group vs. the oe-NC group ($P < 0.05$) but increased in the si-CDC42 group vs. the si-NC group ($P < 0.05$) (Fig. 2E); while invasive cell count showed the opposite trend as cell apoptosis (both $P < 0.05$) (Fig. 2F), which were exhibited by TUNEL and Transwell, respectively (Fig. 2G). According to tube formation assays (Fig. 3A), branch points (Fig. 3B) and tube length (Fig. 3C) were increased in the oe-CDC42 group vs. the oe-NC group (both $P < 0.05$) but reduced in the si-CDC42 group compared to the si-NC group (both $P < 0.05$).

Effect of CDC42 on the MEK/ERK pathway in hRMECs under HG

Immunoblotting was carried out to detect MEK, p-MEK, ERK, and p-ERK in hRMECs under HG (Fig. 4A). It was found that p-MEK/MEK (Fig. 4B) and p-ERK/ERK (Fig. 4C) were increased in the oe-CDC42 group vs. the oe-NC group (both $P < 0.01$); however, they were decreased in the si-CDC42 group vs. the si-NC group (both $P < 0.05$).

Effect of C16-PAF on CDC42-mediated MEK/ERK pathway in hRMECs under HG

CDC42 mRNA level was not different in the C16-PAF group vs. the NC group ($P > 0.05$) and in the si-CDC42 group vs. the si-CDC42 + C16-PAF group ($P > 0.05$) (Fig. 5A). By immunoblotting (Fig. 5B), CDC42 protein exhibited the same trend as CDC42 mRNA (both $P > 0.05$); while p-MEK/MEK and p-ERK/ERK were increased in the C16-PAF group vs. the NC group (both $P < 0.01$), and in

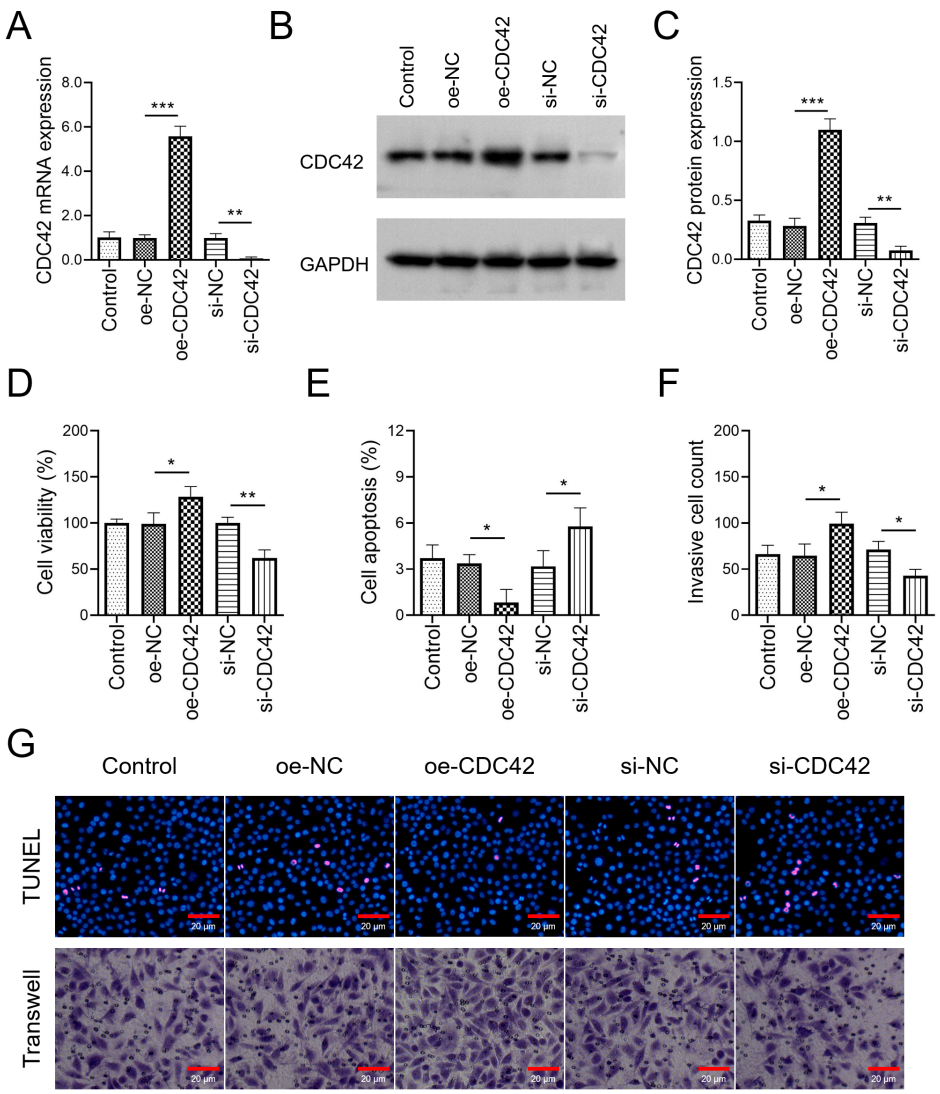

Fig. 2. CDC42 promoted cell viability and invasion but reduced apoptosis in hRMECs under high glucose (HG). CDC42 mRNA (A), representative images of CDC42 protein by immunoblotting (B), CDC42 protein (C), cell viability (D), apoptosis (E), invasive cell count (F), representative images of cell apoptosis and invasion by TUNEL and Transwell assays (G) were compared among the control, oe-NC, oe-CDC42, si-NC, and si-CDC42 groups. The experiments were triplicated. Statistical analysis was performed by one-way ANOVA followed by Tukey's multiple comparison. *$P < 0.05$, **$P < 0.01$, ***$P < 0.001$.

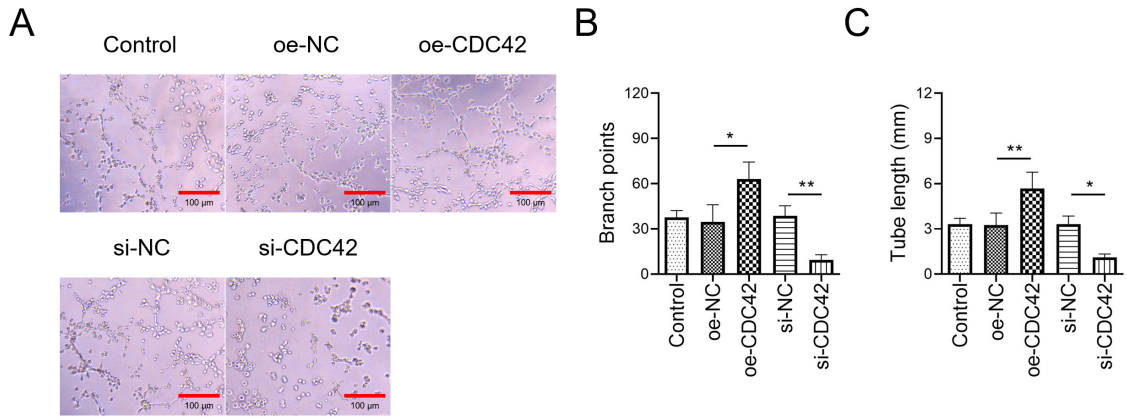

Fig. 3. CDC42 accelerated angiogenesis in hRMECs under high glucose (HG).
Representative images of branch points and tube length by tube formation assay (A), branch points (B) and tube length (C) were compared among the control, oe-NC, oe-CDC42, si-NC, and si-CDC42 groups. The experiments were triplicated. Statistical analysis was performed by one-way ANOVA followed by Tukey's multiple comparison. $*P < 0.05$, $**P < 0.01$.

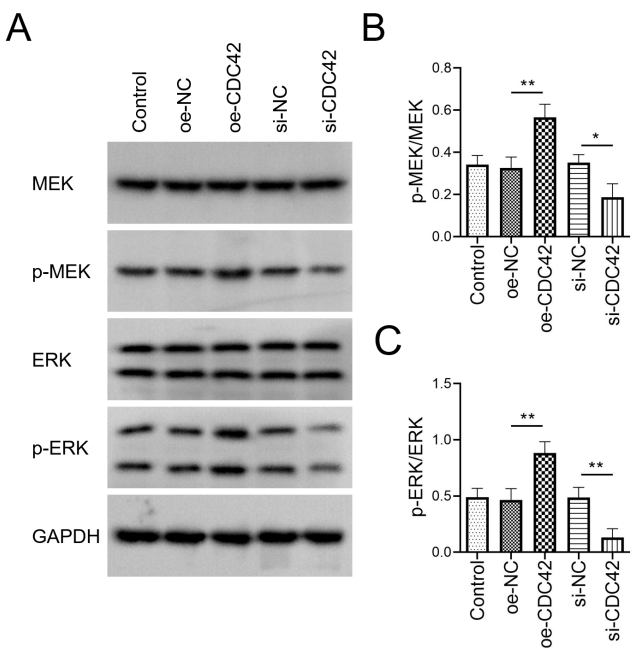

Fig. 4. CDC42 activated MEK/ERK pathway in hRMECs under high glucose (HG).
Representative images of MEK and ERK by immunoblotting (A), and protein levels of p-MEK/MEK (B) and p-ERK/ERK (C) were compared among the control, oe-NC, oe-CDC42, si-NC, and si-CDC42 groups. The experiments were triplicated. Statistical analysis was performed by one-way ANOVA followed by Tukey's multiple comparison. $*P < 0.05$, $**P < 0.01$.

the si-CDC42 + C16-PAF group vs. the si-CDC42 group (both $P < 0.05$) (Fig. 5C).

Effect of C16-PAF on CDC42-mediated cell viability, apoptosis, invasion, and angiogenesis in hRMECs under HG

Cell viability was elevated in the C16-PAF group vs. the NC group ($P < 0.01$), and in the si-CDC42 + C16-PAF group vs. the si-CDC42 group ($P < 0.05$) (Fig. 6A). Cell apoptosis was decreased in the C16-PAF group vs. the NC group ($P < 0.01$), as well as in the si-CDC42 + C16-PAF group compared to the si-CDC42 group ($P < 0.05$) (Fig. 6B), but invasive cell count showed the opposite trend as cell apoptosis (both $P < 0.05$) (Fig. 6C). The representative images for cell apoptosis by TUNEL and invasion by Transwell assays were shown in Fig. 6D. Tube formation assays (Fig. 7A) suggested that branch points (Fig. 7B) and tube length (Fig. 7C) were increased in the C16-PAF group vs. the NC group (both $P < 0.05$), and in the si-CDC42 + C16-PAF group compared to the si-CDC42 group (both $P < 0.05$).

Discussion

HG is one of the major causes of the occurrence and progression of DR, and several studies have disclosed the engagement of HG in DR (Wang et al. 2020; Tan et al. 2021; Huang et al. 2022; Sun et al. 2022). For example, one study elucidates that HG leads to the overexpression of poly (ADP-ribose) polymerase 1 (PARP1) by N6-methyladenosine modification, which further contributes to the progression of DR (Sun et al. 2022). Meanwhile, HG impairs viability, suppresses autophagy, and facilitates cell pyroptosis in retinal pigment epithelial (RPE) cells (Huang et al. 2022). In addition, HG induces cell proliferation, migration, and angiogenesis in hRMECs (Wang et al. 2020). Notably, the current study also found that CDC42 was increased under HG in hRMECs. This finding was partly in line with a previous study, which discovers that CDC42 is upregulated under HG in human renal tubular epithelial cells (Li et al. 2020). The reason behind this might be that HG could induce cytoskeletal reorganization; meanwhile, CDC42 was a key regulatory of cytoskeletal reorganization, which could reflect the cytoskeletal changes (Jiang et al. 2022). Therefore, an increase in CDC42 was observed under the HG condition.

CDC42, as a member of the Rho GTPases family, has been found to be engaged in the development of retinal angiogenesis (Uemura and Fukushima 2021). According to a previous study, the activation of CDC42 facilitates filopodia formation in human retinal endothelial cells (hRECs) (Shen et al. 2021). In addition, VEGF-induced CDC42 activation promotes retinal angiogenesis by enhancing actin polymerization and cell motility in endothelial cells (Kusuhara et al. 2012). Moreover, CDC42 inhibition reduces tip cell and vascular network formation during mouse retinal angiogenesis (Fantin et al. 2015). In the current study, it was found that CDC42 boosted cell viability and invasion, as well as angiogenesis but attenuated cell apoptosis in hRMECs under HG, while the downregulation of CDC42 exhibited an opposite trend. A potential explanation would be that CDC42 might regulate Rho-associated protein kinase (ROCK) and MEK/ERK pathway to enhance cell viability, invasion, and angiogenesis while reducing cell apoptosis, thereby involving in the progression of DR (Tenconi et al. 2019; Shen et al. 2021).

MEK/ERK pathway plays a fundamental role in the pathogenesis of various retinal vascular diseases, including DR (Qin et al. 2013; Tenconi et al. 2019; Hsiao et al. 2021). A previous study indicates that the inhibition of the MEK/ERK pathway regulates human retinal pigment epithelial cell viability and caspase-3 activation under HG (Tenconi et al. 2019). Meanwhile, another study figures out that the blockage of the MEK/ERK pathway inhibits HG-induced human retinal vascular endothelial cell proliferation, migration, and neovascularization (Li and Xiao 2021). Furthermore, the MEK/ERK pathway is also responsible for human RPE cell proliferation, migration, and collagen I expression under HG (Qin et al. 2013). More importantly, one previous study figures out that CDC42 activates the MEK/ERK pathway to regulate angiogenesis (Chen et al. 2021). Partly in line with this previous study (Chen et al. 2021), the present study found that CDC42 positively regulated the MEK/ERK pathway in hRMECs under HG. A possible reason could be that CDC42 could interact with phospholipase D (PLD) and secretogranin III (Scg3) to regulate the MEK/ERK pathway (Jin et al. 2013; Tang et al. 2018; Tenconi et al. 2019). In addition, it was also found that the addition of C16-PAF attenuated the effect of downregulated CDC42 on the MEK/ERK pathway, as well as weakened the implication of downregulated CDC42 on cell viability, invasion, and angiogenesis in hRMECs under HG. The explanation behind this could be that downregulated CDC42 could modulate several proteins (mentioned above) to inhibit MEK/ERK pathway, thereby retarding DR progression (Jin et al. 2013; Tang et al. 2018; Tenconi et al. 2019). However, whether the regulation of CDC42 in the MEK/ERK pathway was direct or indirect should be validated by further experiments.

Notably, anti-VEGF therapy has made some progress in treating DR patients, since VEGF is a key modulatory in DR progression, which promotes retinal endothelial cell proliferation, and its excessive secretion stimulates angiogenesis (Stitt et al. 2016). However, some DR patients still cannot respond well to anti-VEGF therapy, resulting in a poor visual outcome. In this study, it was found that CDC42 could activate the MEK/ERK pathway to participate in the DR progression. Considering the involvement of CDC42 in DR, CDC42 might serve as a potential target in DR patients.

To sum up, CDC42 exacerbates HG-induced hRMEC viability, invasion, and angiogenesis, but attenuates apoptosis by activating the MEK/ERK pathway, which may be responsible for the progression of Dr. These findings sug-

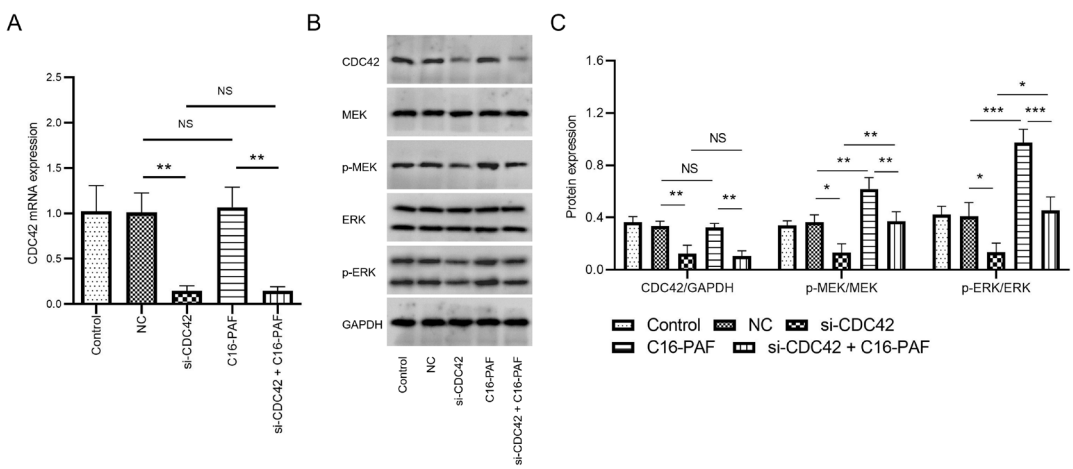

Fig. 5. C16-PAF attenuated the effect of downregulated CDC42 on the MEK/ERK pathway in hRMECs under high glucose (HG).

CDC42 mRNA (A), representative images of CDC42, MEK, and ERK by immunoblotting (B), and protein levels of CDC42, p-MEK/MEK, and p-ERK/ERK (C) were compared among the control, NC, si-CDC42, C16-PAF, and si-CDC42 + C16-PAF groups. The experiments were triplicated. Statistical analysis was performed by one-way ANOVA followed by Tukey's multiple comparison. $*P < 0.05$, $**P < 0.01$, $***P < 0.001$.

gest that targeting CDC42 may be a potential treatment for DR patients.

Acknowledgments

This study was supported by Hunan Provincial Natural Science Foundation of China (2021JJ70063).

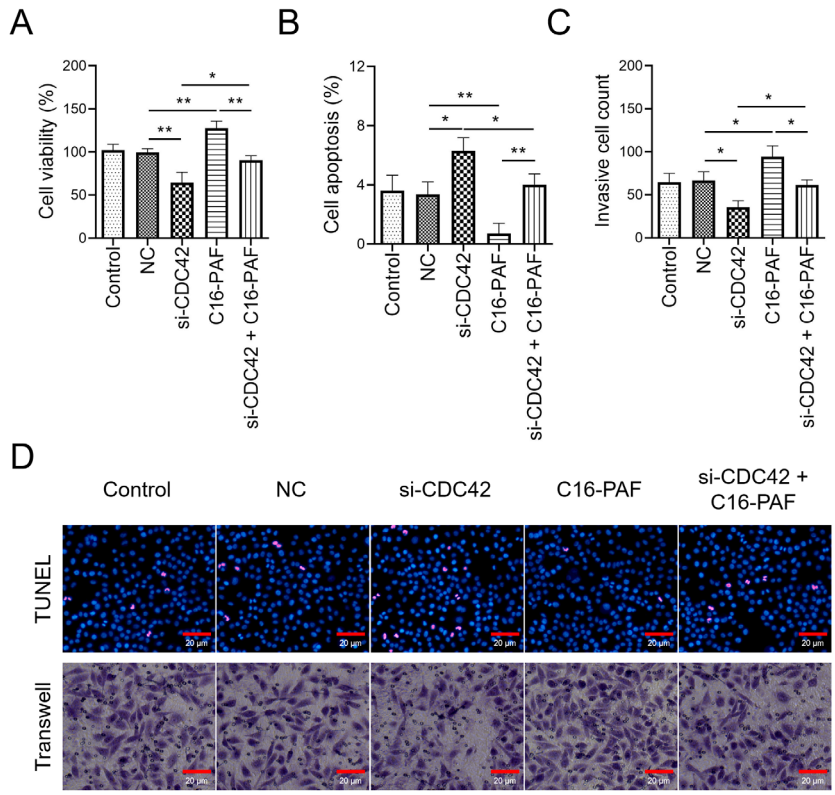

Fig. 6. C16-PAF diminished the effect of downregulated CDC42 on cell viability, apoptosis, and invasion in hRMECs under high glucose (HG).
Cell viability (A), cell apoptosis (B), invasive cell count (C), and representative images of cell apoptosis and invasion by TUNEL and Transwell assays (D) were compared among the control, NC, si-CDC42, C16-PAF, and si-CDC42 + C16-PAF groups. The experiments were triplicated. Statistical analysis was performed by one-way ANOVA followed by Tukey's multiple comparison. $*P < 0.05$, $**P < 0.01$.

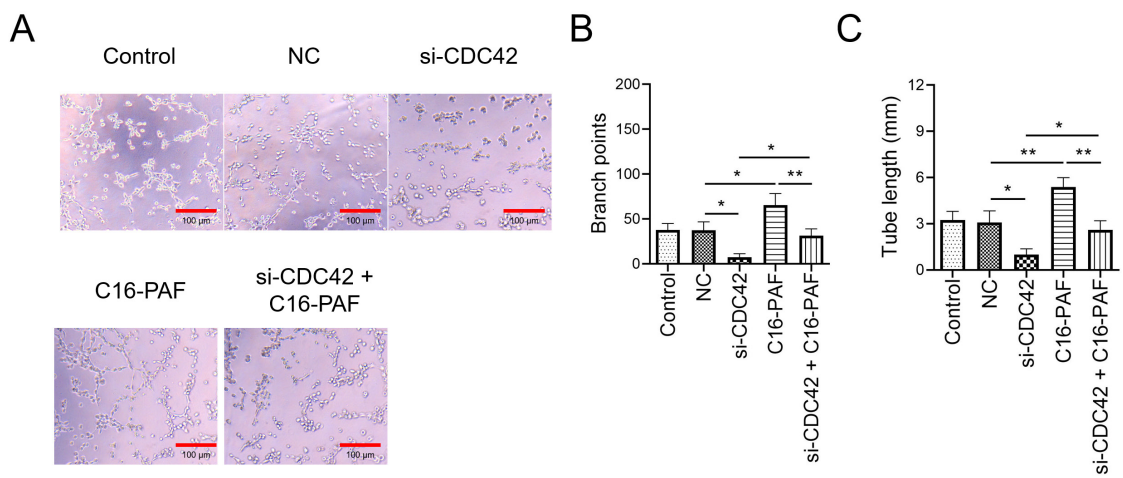

Fig. 7. C16-PAF decreased the effect of downregulated CDC42 on angiogenesis in hRMECs under high glucose (HG).
Representative images of branch points and tube length by tube formation assay (A), branch points (B) and tube length (C) were compared among the control, NC, si-CDC42, C16-PAF, and si-CDC42 + C16-PAF groups. The experiments were triplicated. Statistical analysis was performed by one-way ANOVA followed by Tukey's multiple comparison. $*P < 0.05$, $**P < 0.01$.

Conflict of Interest

The authors declare no conflict of interest.

References

Antonetti, D.A., Silva, P.S. & Stitt, A.W. (2021) Current understanding of the molecular and cellular pathology of diabetic retinopathy. *Nat. Rev. Endocrinol.*, **17**, 195-206.

Chaudhary, S., Zaveri, J. & Becker, N. (2021) Proliferative diabetic retinopathy (PDR). *Dis. Mon.*, **67**, 101140.

Chen, B., Luo, L., Wei, X., Gong, D., Li, Z., Li, S., Tang, W. & Jin, L. (2021) M1 bone marrow-derived macrophage-derived extracellular vesicles inhibit angiogenesis and myocardial regeneration following myocardial infarction via the MALAT1/microRNA-25-3p/CDC42 axis. *Oxid. Med. Cell. Longev.*, **2021**, 9959746.

Everett, L.A. & Paulus, Y.M. (2021) Laser therapy in the treatment of diabetic retinopathy and diabetic macular edema. *Curr. Diab. Rep.*, **21**, 35.

Fantin, A., Lampropoulou, A., Gestri, G., Raimondi, C., Senatore, V., Zachary, I. & Ruhrberg, C. (2015) NRP1 regulates CDC42 activation to promote filopodia formation in endothelial tip cells. *Cell Rep.*, **11**, 1577-1590.

Hsiao, C.C., Chang, Y.C., Hsiao, Y.T., Chen, P.H., Hsieh, M.C., Wu, W.C. & Kao, Y.H. (2021) Triamcinolone acetonide modulates TGF-beta2-induced angiogenic and tissue-remodeling effects in cultured human retinal pigment epithelial cells. *Mol. Med. Rep.*, **24**, 802.

Huang, C., Qi, P., Cui, H., Lu, Q. & Gao, X. (2022) CircFAT1 regulates retinal pigment epithelial cell pyroptosis and autophagy via mediating m6A reader protein YTHDF2 expression in diabetic retinopathy. *Exp. Eye Res.*, **222**, 109152.

Huang, Q.Y., Lai, X.N., Qian, X.L., Lv, L.C., Li, J., Duan, J., Xiao, X.H. & Xiong, L.X. (2019) Cdc42: a novel regulator of insulin secretion and diabetes-associated diseases. *Int. J. Mol. Sci.*, **20**, 179.

Ji, Q., Han, J., Liu, J., Lv, H., Wang, L., Dong, Y. & Shi, L. (2022) LncRNA THRIL promotes high glucose-induced proliferation and migration of human retina microvascular endothelial cells through enhancing autophagy. *Acta Diabetol.*, **59**, 369-380.

Jiang, S., Xu, C.M., Yao, S., Zhang, R., Li, X.Z., Zhang, R.Z., Xie, T.Y., Xing, Y.Q., Zhang, Q., Zhou, X.J., Liao, L. & Dong, J.J. (2022) Cdc42 upregulation under high glucose induces podocyte apoptosis and impairs beta-cell insulin secretion. *Front. Endocrinol.* (*Lausanne*), **13**, 905703.

Jin, J., Yuan, F., Shen, M.Q., Feng, Y.F. & He, Q.L. (2013) Vascular endothelial growth factor regulates primate choroid-retinal endothelial cell proliferation and tube formation through PI3K/Akt and MEK/ERK dependent signaling. *Mol. Cell. Biochem.*, **381**, 267-272.

Khan, R., Chandra, S., Rajalakshmi, R., Rani, P.K., Anantharaman, G., Sen, A., Desai, A., Roy, R., Natarajan, S., Chen, L., Chawla, G., Behera, U.C., Gopal, L., Gurudas, S., Sivaprasad, S., et al. (2020) Prevalence and incidence of visual impairment in patients with proliferative diabetic retinopathy in India. *Sci. Rep.*, **10**, 10513.

Kusuhara, S., Fukushima, Y., Fukuhara, S., Jakt, L.M., Okada, M., Shimizu, Y., Hata, M., Nishida, K., Negi, A., Hirashima, M., Mochizuki, N., Nishikawa, S. & Uemura, A. (2012) Arhgef15 promotes retinal angiogenesis by mediating VEGF-induced Cdc42 activation and potentiating RhoJ inactivation in endothelial cells. *PLoS One*, **7**, e45858.

Lavina, B., Castro, M., Niaudet, C., Cruys, B., Alvarez-Aznar, A., Carmeliet, P., Bentley, K., Brakebusch, C., Betsholtz, C. & Gaengel, K. (2018) Defective endothelial cell migration in the absence of Cdc42 leads to capillary-venous malformations. *Development*, **145**, dev161182.

Li, L., Xu, L., Wen, S., Yang, Y., Li, X. & Fan, Q. (2020) The effect of lncRNA-ARAP1-AS2/ARAP1 on high glucose-induced cytoskeleton rearrangement and epithelial-mesenchymal transition in human renal tubular epithelial cells. *J. Cell. Physiol.*, **235**, 5787-5795.

Li, W. & Xiao, H. (2021) Scutellaria barbata D. Don polysaccharides inhibit high glucose-induced proliferation and angiogenesis of retinal vascular endothelial cells. *Diabetes Metab. SynDr. Obes.*, **14**, 2431-2440.

Liu, Y. & Wu, N. (2021) Progress of nanotechnology in diabetic retinopathy treatment. *Int. J. Nanomedicine*, **16**, 1391-1403.

Purola, P.K.M., Ojamo, M.U.I., Gissler, M. & Uusitalo, H.M.T. (2022) Changes in visual impairment due to diabetic retinopathy during 1980-2019 based on nationwide register data. *Diabetes Care*, **45**, 2020-2027.

Qin, D., Zheng, X.X. & Jiang, Y.R. (2013) Apelin-13 induces proliferation, migration, and collagen I mRNA expression in human RPE cells via PI3K/Akt and MEK/Erk signaling pathways. *Mol. Vis.*, **19**, 2227-2236.

Schreur, V., Brouwers, J., Van Huet, R.A.C., Smeets, S., Phan, M., Hoyng, C.B., de Jong, E.K. & Klevering, B.J. (2021) Long-term outcomes of vitrectomy for proliferative diabetic retinopathy. *Acta Ophthalmol.*, **99**, 83-89.

Shen, J., Rossato, F.A., Cano, I. & Ng, Y.S.E. (2021) Novel engineered, membrane-tethered VEGF-A variants promote formation of filopodia, proliferation, survival, and cord or tube formation by endothelial cells via persistent VEGFR2/ERK signaling and activation of CDC42/ROCK pathways. *FASEB J.*, **35**, e22036.

Shen, J., Wang, R., He, Z., Huang, H., He, X., Zhou, J., Yan, Y., Shen, S., Shao, X., Shen, X., Weng, C., Lin, W. & Chen, J. (2016) NMDA receptors participate in the progression of diabetic kidney disease by decreasing Cdc42-GTP activation in podocytes. *J. Pathol.*, **240**, 149-160.

Stitt, A.W., Curtis, T.M., Chen, M., Medina, R.J., McKay, G.J., Jenkins, A., Gardiner, T.A., Lyons, T.J., Hammes, H.P., Simo, R. & Lois, N. (2016) The progress in understanding and treatment of diabetic retinopathy. *Prog. Retin. Eye Res.*, **51**, 156-186.

Sun, J., Liu, G., Chen, R., Zhou, J., Chen, T., Cheng, Y., Lou, Q. & Wang, H. (2022) PARP1 is upregulated by hyperglycemia via N6-methyladenosine modification and promotes diabetic retinopathy. *Discov. Med.*, **34**, 115-129.

Tan, A., Li, T., Ruan, L., Yang, J., Luo, Y., Li, L. & Wu, X. (2021) Knockdown of Malat1 alleviates high-glucose-induced angiogenesis through regulating miR-205-5p/VEGF-A axis. *Exp. Eye Res.*, **207**, 108585.

Tan, T.E. & Wong, T.Y. (2023) Diabetic retinopathy: looking forward to 2030. *Front. Endocrinol.* (*Lausanne*), **13**, 1077669.

Tang, F., Pacheco, M.T.F., Chen, P., Liang, D. & Li, W. (2018) Secretogranin III promotes angiogenesis through MEK/ERK signaling pathway. *Biochem. Biophys. Res. Commun.*, **495**, 781-786.

Tenconi, P.E., Bermudez, V., Oresti, G.M., Giusto, N.M., Salvador, G.A. & Mateos, M.V. (2019) High glucose-induced phospholipase D activity in retinal pigment epithelium cells: new insights into the molecular mechanisms of diabetic retinopathy. *Exp. Eye Res.*, **184**, 243-257.

Teo, Z.L., Tham, Y.C., Yu, M., Chee, M.L., Rim, T.H., Cheung, N., Bikbov, M.M., Wang, Y.X., Tang, Y., Lu, Y., Wong, I.Y., Ting, D.S.W., Tan, G.S.W., Jonas, J.B., Sabanayagam, C., et al. (2021) Global prevalence of diabetic retinopathy and projection of burden through 2045: systematic review and meta-analysis. *Ophthalmology*, **128**, 1580-1591.

Uemura, A. & Fukushima, Y. (2021) Rho GTPases in retinal vascular diseases. *Int. J. Mol. Sci.*, **22**, 3684.

Wang, L., Liu, W.X. & Huang, X.G. (2020) MicroRNA-199a-3p inhibits angiogenesis by targeting the VEGF/PI3K/AKT signalling pathway in an in vitro model of diabetic retinopathy. *Exp. Mol. Pathol.*, **116**, 104488.

Whitehead, M., Wickremasinghe, S., Osborne, A., Van Wijngaarden, P. & Martin, K.R. (2018) Diabetic retinopathy: a complex pathophysiology requiring novel therapeutic strategies. *Expert Opin. Biol. Ther.*, **18**, 1257-1270.

Xia, T., Ma, J., Sun, Y. & Sun, Y. (2022) Androgen receptor suppresses inflammatory response of airway epithelial cells in allergic asthma through MAPK1 and MAPK14. *Hum. Exp. Toxicol.*, **41**, 9603271221121320.

You, D., Qiao, Q., Ono, K., Wei, M., Tan, W., Wang, C., Liu, Y., Liu, G. & Zheng, M. (2022) miR-223-3p inhibits the progression of atherosclerosis via down-regulating the activation of MEK1/ERK1/2 in macrophages. *Aging* (*Albany N. Y.*), **14**, 1865-1878.

Yuan, J.S., Reed, A., Chen, F. & Stewart, C.N. Jr. (2006) Statistical analysis of real-time PCR data. *BMC Bioinformatics*, **7**, 85.